Hidden prompt splashing by corona splashing at drop impact on a smooth dry surface

Taku Ashida, Masao Watanabe ⬤,* Kazumichi Kobayashi ⬤, and Hiroyuki Fujii ⬤
Division of Mechanical and Space Engineering, Hokkaido University, Sapporo 060-8628, Japan

Toshiyuki Sanada ⬤
Department of Mechanical Engineering, Shizuoka University, Hamamatsu 432-8561, Japan

We present the experimental evidence of prompt splashing due to surface roughness at drop impact on a dry smooth surface, by suppressing corona splashing due to the surrounding gas. Prompt splashing occurs during a very early stage of the impact process, and it cannot be suppressed by reducing the gas pressure even to 0.8 kPa. We evaluate the conditions under which corona splashing hides prompt splashing at atmospheric conditions. We also demonstrate the importance of the distinction of two events, i.e., prompt splashing occurs and it can be clearly distinguished.

I. INTRODUCTION

An understanding of high-speed liquid drop impact is required in a number of practical situations, such as thermal spray coating [1–3], spray cooling [4,5], cleaning of surfaces [6], and ink-jet printing [7]. When the impact velocity V of a liquid drop on a solid surface is sufficiently large, the drop splashes, i.e., breaks up and ejects smaller daughter droplets [8,9]. Splashing generally influences industrial outcomes, e.g., it degrades the quality of coating because it leaves voids in the deposit, thereby increasing its porosity and reducing its strength [1]. Hence, significant efforts have been devoted to understanding the mechanisms of drop splashing on a solid surface.

Drop splashing can be generally classified into two types [10], based on descriptive interpretations. "Prompt splashing" occurs at a very early stage of the impact process and is characterized by the generation of droplets directly at the contact line. "Corona splashing" occurs at a later stage of the impact process and is characterized by the formation of droplets around the rim of a corona, remote from the solid surface [8–19]. Two mechanisms for splashing were identified by Xu *et al.* [14], based on physical interpretations. Surface roughness is responsible for prompt splashing and the surrounding gas pressure is responsible for corona splashing. We implement the classification by Xu *et al.* [14] to distinguish between the two types of splashing.

However, it was also reported that reducing the surrounding gas pressure P inhibits not only corona splashing [13], but also prompt splashing [16]. This finding may indicate that splashing does not occur when P is sufficiently low, or a possible ambiguity in the distinction between prompt splashing from corona splashing exists. The implemented classification may eliminate this ambiguity.

In this Rapid Communication, we explore the possibility of prompt splashing on a smooth surface for low Ohnesorge number drops (Oh $\lesssim 0.01$) at a higher impact velocity than previously

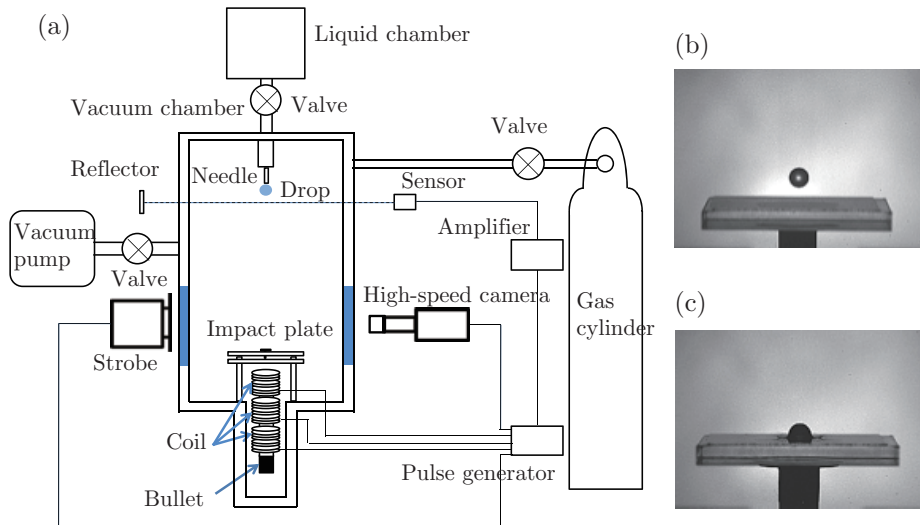---

*masao.watanabe@eng.hokudai.ac.jp

FIG. 1. (a) Sketch of the experimental setup. (b) Free-falling drop and projected solid surface at 112 μs before collision. (c) Drop impact with a solid surface at 48 μs after collision.

considered. We also examine the suppression of prompt splashing under significantly low P conditions, and then discuss the required criterion. The Weber, Reynolds, and Ohnesorge numbers of the impact are defined as We $= \rho V^2 D/\sigma$, Re $= \rho V D/\mu$, and Oh $= \sqrt{\text{We}}/\text{Re}$, where D is the drop diameter and ρ, σ, and μ are the density, surface tension, and dynamic viscosity of the liquid, respectively.

II. EXPERIMENTS

The experimental configuration is shown in Fig. 1(a). A water drop was released from a needle with an inner diameter of 0.22 mm (Terumo needle 27G). The free-falling drop subsequently collided with a vertical traveling impact plate that was projected by an iron bullet that was accelerated by a coilgun. The impact plate consisted of a cover glass (Matsunami Glass Ind., Ltd., 18×18) with a static contact angle $\sim 60°$ and an arithmetic mean roughness (R_a) of the surface ~ 2.1 nm that was adhered to an acrylic plate.

The impact of a freely falling water drop of diameter $D = 2.2 \pm 0.2$ mm with a vertical traveling impact plate [Fig. 1(b)] in a stainless vacuum chamber with transparent polycarbonate observation windows was observed using a long-distance microscope with a resolution of 16.1 μm/px. The typical configuration of a free-falling drop and a projected solid surface are shown in Figs. 1(b) and 1(c) at 112 μs before collision and at 48 μs after collision, respectively. The pressure in the vacuum chamber with an internal volume of 7.9×10^{-3} m^3 was reduced by a vacuum pump (GLD-201B: ULVAC KIKO, Inc.). The surrounding gas pressure P, i.e., the pressure in the vacuum chamber, was measured with a pressure transducer (628F13TDE1B: MKS Instruments, Inc.) and was varied between 0.8 and 104.3 kPa (absolute pressure). The relative impact velocity V was varied between 4.2 and 33 m/s, where the free-fall velocity of the drop was 1.5 m/s at collision [Fig. 1(c)].

The impact of a drop on a solid surface with high relative impact velocity and the subsequent splashing was recorded using a Shimadzu HPV-1 high-speed video camera at 1 Mfps. We used only the experimental results obtained under the conditions where the impact plate was tilted at less than 2° because the tilt of the impact plate affects the splash [20]. We also used only the experimental results for which a circular symmetrical splash was observed. The velocity of the impact plate was evaluated by typically using the nine consecutive positions of the impact plate
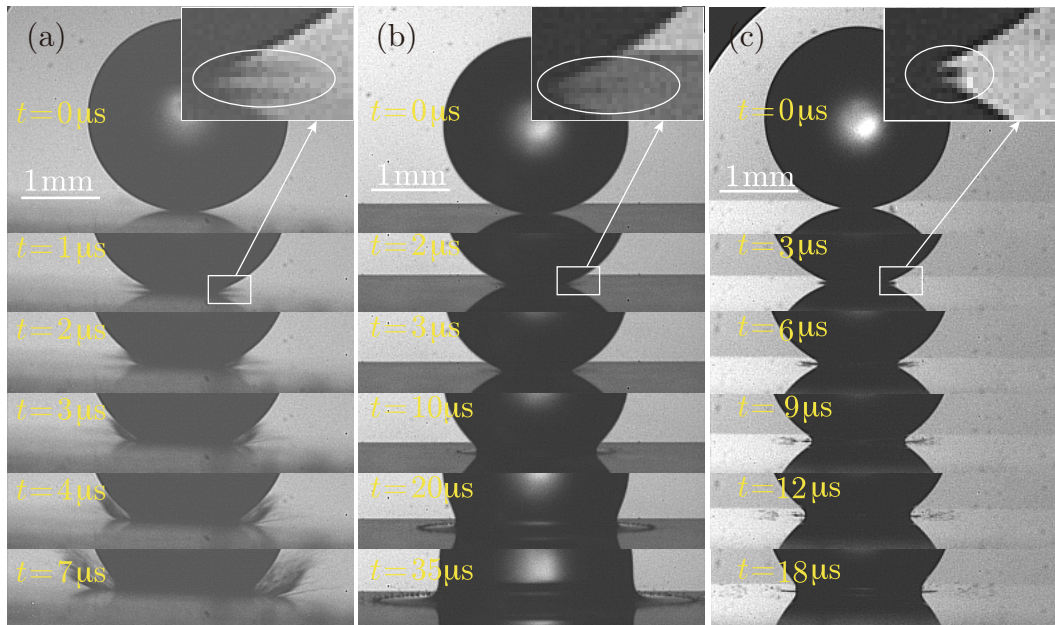
FIG. 2. Splashing after impact. (a) Type-I and type-III splashing: $P = 75.1$ kPa, $V = 25.8$ m/s, and $D = 2.42$ mm. (b) Type-II and type-III splashing: $P = 64.5$ kPa, $V = 14.8$ m/s, and $D = 2.35$ mm. (c) Type-III splashing with subsequent smooth liquid film flow: $P = 0.8$ kPa, $V = 9.64$ m/s, and $D = 2.27$ mm. A magnified image of type-III splashing is also shown in the rectangle in the upper right corner of each image. Movies 1, 2, and 3 in the Supplemental Material [22] correspond to (a), (b), and (c), respectively.

just before the impact and the linear regression method. We found that the impact plate flew at the constant speed in the spatial and temporal accuracy of the present experiment. The possible effects of evaporation/condensation were also addressed [21].

III. RESULTS AND DISCUSSION

Three types of splashing were identified as shown in Fig. 2. The first type is represented in Fig. 2(a) and Movie 1 in the Supplemental Material [22]. Straight filaments of liquid (fingers) were ejected with an initial outward angle [15]; then, those filaments disintegrated into multiple secondary droplets traveling obliquely upward. This is referred to as "type-I splashing." This splashing is similar to that previously identified as prompt splashing [15].

The second type is represented in Fig. 2(b) and Movie 2. A film flow along the surface with a disturbed rim developed; then, multiple secondary droplets were ejected from the rim. This is referred to as "type-II splashing." The distinguishable characteristic of this splashing compared to type-I splashing is that neither the formation of fingers nor dewetting of the solid were observed. This splashing is similar to that also previously identified as prompt splashing [16–19].

The third type is represented not only in Fig. 2(c), but also in Figs. 2(a) and 2(b). In Fig. 2(c) and Movie 3, fast-moving fine droplets, possibly smaller than those observed for the other two types, traveled along the solid surface immediately after impact before a smooth liquid film flow was developed. This is referred to as "type-III splashing." Type-III splashing can be clearly distinguished from the other two types. Indeed, type-III splashing and the other two types were observed separately. Preceding type-I or type-II splashing, type-III splashing was observed immediately after impact, as represented by the rectangles in the upper right corner of Figs. 2(a) and 2(b), and Movies 1 and 2.
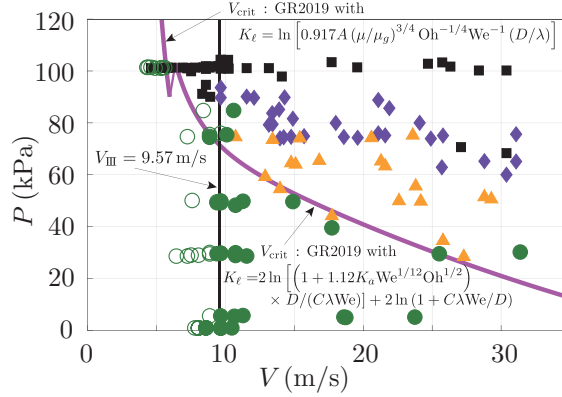
FIG. 3. Various types of splashing with respect to V and P: Type-I corona and type-III splashing ($\blacklozenge$), type-II corona and type-III splashing ($\blacktriangle$), type-III splashing with subsequent smooth liquid film flow ($\bullet$), no splashing ($\circ$), and indistinguishable ($\blacksquare$). The threshold velocity of type-III splashing is $V_{\mathrm{III}} = 9.57\,\mathrm{m/s}$ (navy blue $- - -$). The predicted critical velocity V_{crit} (magenta $- - -$) was calculated using the criterion proposed in GR2019 [23]. In the limit $\mathrm{We}(2\lambda/D) \ll (\mu_g/\mu)^{3/4}\,\mathrm{Oh}^{1/4}$, where μ_g is the gas viscosity and λ is the mean free path of the gas molecules, the expression for K_ℓ can be given as $K_\ell = \ln[0.917A(\mu/\mu_g)\mathrm{Oh}^{-1/4}\,\mathrm{We}^{-1}(D/\lambda)]$, where A is a fitting constant. However, when $\mathrm{We}(2\lambda/D) \gtrsim (\mu_g/\mu)^{3/4}\,\mathrm{Oh}^{1/4}$, the expression for K_ℓ is given by $K_\ell = 2\ln[(1 + 1.12K_a\,\mathrm{We}^{1/12}\,\mathrm{Oh}^{1/2})D/(C\lambda\mathrm{We})] + 2\ln(1 + C\lambda\,\mathrm{We}/D)$, where K_a is a proportionality constant and C is a fitting constant. In the calculation, $A = 0.011$, $C = 10$, and $K_a = 0.5$ were used.

The occurrence of these splashings is shown with respect to V and P in Fig. 3. Type-I and type-II splashing depend on the surrounding gas pressure while type-III splashing does not. Indeed, the reduction of P to even 0.8 kPa does not suppress type-III splashing. Note that type-I and type-II splashing are completely suppressed when P is sufficiently low for a given V as represented in Movie 4, where $P = 29.5$ kPa, $V = 25.5$ m/s, and $D = 2.16$ mm.

To better understand type-I and type-II splashing, we examine whether they can be predicted using the criterion for splashing, for which the surrounding gas is responsible, proposed by Gordillo and Riboux [23]. This criterion was determined from the condition for the case of low-viscosity liquids ($\mathrm{Re}^{1/6}\,\mathrm{Oh}^{2/3} < 0.223$) and millimetric droplets, $(K_\ell\,\mu_g\,V/\sigma) = 0.0584\,\mathrm{We}^{-1/3} - 0.0796(\rho_g/\rho)\mathrm{We}^{1/3}$, where μ_g and ρ_g are the gas viscosity and density, respectively, and K_ℓ is a coefficient presented in Fig. 3.

The critical velocity V_{crit} for surrounding-gas-dependent splashing was calculated and plotted in Fig. 3. It is evident that neither type-I nor type-II splashing occurs below V_{crit}. This implies that the surrounding gas is responsible for these splashings. Given that we have implemented the classification by Xu *et al.* [14], type-I and type-II splashing are identified as corona splashing. Note that the formation of neither a curved film, nor a crown, entailed by secondary droplets emitted from the outer rim was observed in type-I corona splashing. In addition, no formation of upwardly curved fingers in type-II corona splashing was observed.

In contrast to corona splashing, type-III splashing is independent of P as shown in Movies 3, 5, 6, and 7, where type-III splashing at $P = 0.8$, 5.7, 28.8, and 49.8 kPa with $V \approx 10$ m/s are represented, respectively. Type-III splashing is always observed above V_{III} up to $P \lesssim 90$ kPa and has a constant value of $V_{\mathrm{III}} = 9.57$ m/s for a water drop with a diameter of 2.20 mm, as shown in Fig. 3. Further examination of the effect of the surrounding gas is provided in the Supplemental Material [22] and the references therein [24–29]. The threshold velocity V_{III} is also independent of the species of the surrounding gas.

To identify type-III splashing, we examine the criteria for type-III splashing. Splashing criteria have often been expressed as a power law, typically the product of an exponentiated We or Re, and
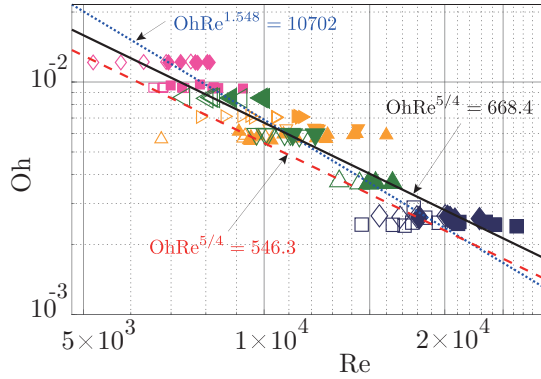
FIG. 4. Criteria for type-III splashing for various liquids and drop diameters represented by the critical Oh as a function of Re: $\mathrm{Oh}\,\mathrm{Re}^{1.548} = 10\,702$ (....), $\mathrm{Oh}\,\mathrm{Re}^{5/4} = 668.4$ (___), $\mathrm{Oh}\,\mathrm{Re}^{5/4} = 546.3$ (- - -). The solid and open symbols indicate whether or not prompt splashing is observed, respectively.

Oh. They can be rewritten in terms of a "splashing parameter" [30] $K = \mathrm{Oh}\,\mathrm{Re}^{\chi}$, where K and χ are empirically determined constants.

To test whether type-III splashing criteria can be expressed as a power law, we investigated this type of splashing for a varieties of liquids as shown in Fig. 4. The physical properties of these liquids and experimental conditions are listed in Tables II–V in the Supplemental Material [22] and the references therein [31–34]. We evaluated the splashing parameter to obtain $\mathrm{Oh}\,\mathrm{Re}^{1.548} = 10\,702$. Since this scaling behavior is similar to that proposed by Refs. [11,12], it can be approximated as follows [35],

$$\mathrm{Oh}\,\mathrm{Re}^{5/4} = K_{\mathrm{p}}, \tag{1}$$

where $K_{\mathrm{p}} = 668.4$. It is well known that the splashing parameter K_{p} for the power law with $\chi = 5/4$ can be evaluated by an empirical correlation [36] that used experimental results [11,12],

$$K_{\mathrm{p}} = \left(649 + 3.76\,S_a^{-0.63}\right)^{5/8}, \tag{2}$$

in the range that $1.35 \times 10^{-5} \leqslant S_a \leqslant 0.86$, where S_a ($S_a = R_a/D$) is the nondimensional roughness and R_a is the mean roughness of the solid surface. A typical value for K_{p} calculated using Eq. (2) in our experiment was 546.3 for $S_a = 9.546 \times 10^{-7}$.

Equations (1) and (2) represent the criteria for splashing for which the surface roughness is responsible; hence the surface roughness is also responsible for type-III splashing. Given that we have implemented the classification by Ref. [14], type-III splashing is identified as prompt splashing. Note that Eq. (2) is an empirical correlation; hence, further investigations are required to describe the role of the characteristics of the surface more accurately [30].

Since type-III splashing is identified as prompt splashing, we can conclude that we successfully acquired the experimental evidence that prompt splashing occurs on a smooth surface ($R_a = 2.1$ nm). However, the results of previous experiments indicated that prompt splashing does not occur if the roughness is too small [14]. The use of a high-speed camera with a significantly high temporal resolution facilitated the observation of prompt splashing on a smooth surface.

Our results also imply that prompt splashing cannot be suppressed by reducing the surrounding gas pressure P to 0.8 kPa when V is greater than the threshold velocity. However, the results of previous experiments indicated that reducing P inhibits prompt splashing [16]. Comparing our results to previously published findings, the importance of the elapsed time t_{p} from impact to the occurrence of prompt splashing is realized. The nondimensional elapsed time t_{p}^* ($= t_{\mathrm{p}} V/D$) used in the previous studies are significantly larger than ours. The results by Stow and Hadfield [11] and ours indicate that prompt splashing occurs at a very early stage of the impact process, i.e., $t_{\mathrm{p}}^* < 0.1$.
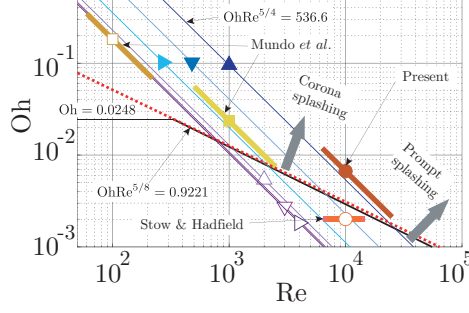
FIG. 5. Criteria for corona splashing at atmospheric conditions are plotted with the criteria for prompt splashing: $\mathrm{Oh\,Re}^{0.609} = 0.8458$ [35] $(\cdots)$; $\mathrm{Oh\,Re}^{5/8} = 0.207(\mu/\mu_g)^{3/8}$ [37] (—). Criteria for prompt splashing are plotted: $\mathrm{Oh\,Re}^{1.25} = K_\mathrm{p}$ [12] with Eq. (2) for $S_a = 1.0 \times 10^{-6}$ (—▲—), $S_a = 1.0 \times 10^{-5}$ (—▼—), $S_a = 1.0 \times 10^{-4}$ (—▶—), $S_a = 1.0 \times 10^{-3}$ (—△—), $S_a = 1.0 \times 10^{-2}$ (—▽—), and $S_a = 1.0 \times 10^{-1}$ (—▷—). The ranges of our experimental results (Fig. 4) are plotted (—●—), with those of previous experimental results: Stow and Hadfield [11] (—○—); Mundo *et al.* [12] (—□—) and (—■—).

This suggests that the splashing observed on a rough surface with larger t_p^* [16–19] may not have been prompt splashing.

Figures 2(a) and 2(b) show that prompt splashing occurs regardless of whether corona splashing occurs. Prompt and corona splashing occur independently of each other. However, prompt splashing cannot be clearly distinguished from corona splashing when $P \gtrsim 90$ kPa as shown in Movies 8 and 9. This ambiguity in the distinction between prompt splashing and corona splashing may have contaminated the classification of prompt splashing in the previous studies. Corona splashing may hide prompt splashing although prompt splashing occurs at atmospheric conditions.

Therefore, we examine this possibility. The criteria for corona splashing at atmospheric conditions were investigated. It is essential to distinguish the two events, i.e., prompt splashing occurs and it can be clearly distinguished.

At atmospheric conditions, the threshold velocity V_c for surrounding-gas-dependent splashing for small Oh drops has been proposed $V_\mathrm{c} = 0.080\,34\,\sigma^{4/5}\mu_g^{-3/5}(\rho D)^{-1/5}$ [37], by approximating the criterion proposed by Riboux and Gordillo [38]. Given that surrounding-gas-dependent splashing is classified as corona splashing [14], the criterion for corona splashing for small Oh drops at atmospheric conditions can be written as

$$\mathrm{Oh\,Re}^{5/8} = K_\mathrm{c}, \text{ where } K_\mathrm{c} = 0.207(\mu/\mu_g)^{3/8}. \tag{3}$$

Substituting the water and air viscosities in Eq. (3), $K_\mathrm{c} = 0.9221$. This scaling behavior is similar to the empirical splashing boundary: $\mathrm{Oh\,Re}^{0.6089} = 0.8458$ [35]. Considering that Eq. (3) defines the criterion for corona splashing at atmospheric conditions, it can be inferred that this empirical criterion may have applied to corona splashing.

It is widely known that the existing criteria for splashing can be divided into (at least) two groups [39]. The explanation for the two distinct splashings by Xu *et al.* [14] can provide a rationale for the existence of these groups. The first group with $\chi = 5/4$ provides the criterion for the prompt splashing, i.e., Eq. (1). The second group with $\chi \leqslant 1$, or more precisely $\chi = 5/8$, provides the criterion for corona splashing, i.e., Eq. (3).

Figure 5 indicates that corona splashing at atmospheric conditions occurs when $\mathrm{Oh\,Re}^{5/8} > K_\mathrm{c}$ and prompt splashing occurs when $\mathrm{Oh\,Re}^{5/4} > K_\mathrm{p}$. The previous experiments [11] suggest that prompt splashing can be clearly distinguished when the conditions $\mathrm{Oh\,Re}^{5/8} < K_\mathrm{c}$ and $\mathrm{Oh\,Re}^{5/4} > K_\mathrm{p}$ are satisfied. As shown in Movies 8 and 9, the distinction between prompt splashing and corona splashing may not be as clear when the conditions $\mathrm{Oh\,Re}^{5/8} > K_\mathrm{c}$ and $\mathrm{Oh\,Re}^{5/4} > K_\mathrm{p}$ are satisfied at atmospheric conditions. Corona splashing may hide prompt splashing until the surrounding gas

pressure is sufficiently reduced, as demonstrated in our experiments conducted under the condition $\mathrm{Oh} \lesssim 0.01$.

However, Mundo *et al.* [12] observed splashing that satisfies the criterion for prompt splashing [Eqs. (1) and (2)] under the conditions $\mathrm{Oh}\,\mathrm{Re}^{5/8} > K_\mathrm{c}$, where corona splashing is predicted to be dominant at atmospheric conditions, as shown in Fig. 5. Considering our results, they should have observed both corona and prompt splashing; however, a description of two distinct types of splashing was not provided. Note that Eq. (3) is valid only for $\mathrm{Re}^{1/6}\,\mathrm{Oh}^{2/3} < 0.223$ [37,40], i.e., $\mathrm{Oh} < 0.0248$. The results of the experiments that can support the validity of Eq. (3) are available for $\mathrm{Oh} \lesssim 0.015$ [35]. Considering these and our results, our description of the dominance of corona splashing over prompt splashing at atmospheric conditions may apply to only low Oh drops ($\mathrm{Oh} \lesssim 0.01$). This suggests that splashing criteria for higher Oh drops ($\mathrm{Oh} > 0.01$) should be further investigated.

In this Rapid Communication, we have provided the experimental evidence that prompt splashing occurs on a dry smooth solid surface for low Oh drops ($\mathrm{Oh} \lesssim 0.01$) using a 1-Mfps high-speed video camera. We demonstrated that the previously proposed splashing criterion can predict prompt splashing even on a smooth surface; however, the empirical correlation Eq. (2) should be further investigated to more accurately describe the role of the characteristics of the surface. We also characterized prompt splashing based on its occurrence at a very early stage of the impact process ($t^* \lesssim 0.1$), and by its independence of the surrounding gas pressure P; prompt splashing cannot be suppressed by reducing P. Further, we have demonstrated the importance of the distinction of the two events, i.e., prompt splashing occurs and it can be clearly distinguished. In addition, we proposed the possibility that corona splashing may hide prompt splashing.

ACKNOWLEDGMENTS

---

[1] S. D. Aziz and S. Chandra, Impact, recoil and splashing of molten metal droplets, Int. J. Heat Mass Transfer **43**, 2841 (2000).

[2] K. K. Haller, Y. Ventikos, D. Poulikakos, and P. Monkewitz, Computational study of high-speed liquid droplet impact, J. Appl. Phys. **92**, 2821 (2002).

[3] Y. Wang, Y. Bai, K. Wu, J. Zhou, M. G. Shen, W. Fan, H. Y. Chen, Y. X. Kang, and B. Q. Li, Flattening and solidification behavior of in-flight droplets in plasma spraying and micro/macro-bonding mechanisms, J. Alloys Compd. **784**, 834 (2019).

[4] G. Liang and I. Mudawar, Review of spray cooling - Part 1: Single-phase and nucleate boiling regimes, and critical heat flux, Int. J. Heat Mass Transfer **115**, 1174 (2017).

[5] G. Liang and I. Mudawar, Review of spray cooling - Part 2: High temperature boiling regimes and quenching applications, Int. J. Heat Mass Transfer **115**, 1206 (2017).

[6] T. Sanada and M. Watanabe, Photoresist and thin metal film removal by steam and water mixed spray, J. Photopolym. Sci. Technol. **28**, 289 (2015).

[7] D. B. van Dam and C. Le Clerc, Experimental study of the impact of an ink-jet printed droplet on a solid substrate, Phys. Fluids **16**, 3403 (2004).

[8] A. L. Yarin, Drop impact dynamics: Splashing, spreading, receding, bouncing, Annu. Rev. Fluid Mech. **38**, 159 (2006).

[9] C. Josserand and S. T. Thoroddsen, Drop impact on a solid surface, Annu. Rev. Fluid Mech. **48**, 365 (2016).

[10] R. Rioboo, C. Tropea, and M. Marengo, Outcomes from a drop impact on solid surfaces, Atomization Sprays **11**, 155 (2001).

[11] C. Stow and M. Hadfield, An experimental investigation of fluid flow resulting from the impact of a water drop with an unyielding dry surface, Proc. R. Soc. London, Ser. A **373**, 419 (1981).

[12] C. Mundo, M. Sommerfeld, and C. Tropea, Droplet-wall collisions: Experimental studies of the deformation and breakup process, Int. J. Multiphase Flow **21**, 151 (1995).

[13] L. Xu, W. W. Zhang, and S. R. Nagel, Drop Splashing on a Dry Smooth Surface, Phys. Rev. Lett. **94**, 184505 (2005).

[14] L. Xu, L. Barcos, and S. R. Nagel, Splashing of liquids: Interplay of surface roughness with surrounding gas, Phys. Rev. E **76**, 066311 (2007).

[15] K.-L. Pan, K.-C. Tseng, and C.-H. Wang, Breakup of a droplet at high velocity impacting a solid surface, Exp. Fluids **48**, 143 (2010).

[16] A. Latka, A. Strandburg-Peshkin, M. M. Driscoll, C. S. Stevens, and S. R. Nagel, Creation of Prompt and Thin-Sheet Splashing by Varying Surface Roughness or Increasing Air Pressure, Phys. Rev. Lett. **109**, 054501 (2012).

[17] I. V. Roisman, A. Lembach, and C. Tropea, Drop splashing induced by target roughness and porosity: The size plays no role, Adv. Colloid Interface Sci. **222**, 615 (2015).

[18] C. Tang, M. Qin, X. Weng, X. Zhang, P. Zhang, J. Li, and Z. Huang, Dynamics of droplet impact on solid surface with different roughness, Int. J. Multiphase Flow **96**, 56 (2017).

[19] J. Hao, Effect of surface roughness on droplet splashing, Phys. Fluids **29**, 122105 (2017).

[20] J. Liu, H. Vu, S. S. Yoon, R. Jepsen, and G. Aguilar, Splashing phenomena during liquid droplet impact, Atomization Sprays **20**, 297 (2010).

[21] E. Q. Li, K. R. Langley, Y. S. Tian, P. D. Hicks, and S. T. Thoroddsen, Double Contact During Drop Impact on a Solid under Reduced Air Pressure, Phys. Rev. Lett. **119**, 214502 (2017).

[22] See Supplemental Material at http://link.aps.org/supplemental/10.1103/PhysRevFluids.5.011601 for the description of the supplemental movies, for the physical properties of liquids used and experimental conditions in Fig. 4, and for a discussion on the effect of surrounding gas on prompt splashing.

[23] J. M. Gordillo and G. Riboux, A note on the aerodynamic splashing of droplets, J. Fluid Mech. **871**, 1 (2019).

[24] R. C. A. van der Veen, T. Tran, D. Lohse, and C. Sun, Direct measurements of air layer profiles under impacting droplets using high-speed color interferometry, Phys. Rev. E **85**, 026315 (2012).

[25] P. D. Hicks and R. Purvis, Air cushioning in droplet impacts with liquid layers and other droplets, Phys. Fluids **23**, 062104 (2011).

[26] E. Q. Li, I. U. Vakarelski, and S. T. Thoroddsen, Probing the nanoscale: The first contact of an impacting drop, J. Fluid Mech. **785**, R2 (2015).

[27] S. Mandre, M. Mani, and M. P. Brenner, Precursors to Splashing of Liquid Droplets on a Solid Surface, Phys. Rev. Lett. **102**, 134502 (2009).

[28] S. Mandre and M. P. Brenner, The mechanism of a splash on a dry solid surface, J. Fluid Mech. **690**, 148 (2012).

[29] L. Duchemin and C. Josserand, Rarefied gas correction for the bubble entrapment singularity in drop impacts, C. R. Mec. **340**, 797 (2012).

[30] A. L. N. Moreira, A. S. Moita, and M. R. Panão, Advances and challenges in explaining fuel spray impingement: How much of single droplet impact research is useful? Prog. Energy Combust. Sci. **36**, 554 (2010).

[31] H. Uchida, *JSME Data Book: The Thermophysical Properties of Fluids* (The Japan Society of Mechanical Engineers, Tokyo, 1983), Chap. 2.

[32] I. S. Khattab, F. Bandakarr, M. A. A. Fakhree, and A. Jouyban, Density, viscosity, and surface tension of water+ethanol mixtures from 293 to 323 K, Korean J. Chem. Eng. **29**, 812 (2012).

[33] H. S. Ashbaugh, J. Wesley Barnett, A. Saltzman, M. E. Langrehr, and H. Houser, Communication: Stiffening of dilute alcohol and alkane mixtures with water, J. Chem. Phys. **145**, 201102 (2016).

[34] N. V. Sastry and M. K. Valand, Densities, speeds of sound, viscosities, and relative permittivities for 1-propanol + and 1-butanol + heptane at 298.15 K and 308.15 K, J. Chem. Eng. Data **41**, 1421 (1996).

[35] R. L. Vander Wal, G. M. Berger, and S. D. Mozes, The splash/non-splash boundary upon a dry surface and thin fluid film, Exp. Fluids **40**, 53 (2005).

[36] G. E. Cossali, A. Coghe, and M. Marengo, The impact of a single drop on a wetted solid surface, Exp. Fluids **22**, 463 (1997).

[37] T. C. de Goede, N. Laan, K. G. de Bruin, and D. Bonn, Effect of wetting on drop splashing of Newtonian fluids and blood, Langmuir **34**, 5163 (2018).

[38] G. Riboux and J. M. Gordillo, Experiments of Drops Impacting a Smooth Solid Surface: A Model of the Critical Impact Speed for Drop Splashing, Phys. Rev. Lett. **113**, 024507 (2014).

[39] M. Rein and J.-P. Delplanque, The role of air entrainment on the outcome of drop impact on a solid surface, Acta Mech. **201**, 105 (2008).

[40] G. Riboux and J. M. Gordillo, Boundary-layer effects in droplet splashing, Phys. Rev. E **96**, 013105 (2017).